ELSEVIER

Journal of Chromatography A, 679 (1994) 1–9

JOURNAL OF CHROMATOGRAPHY A

Frontal analysis of protein adsorption on a membrane adsorber

Ayahito Shiosaki, Motonobu Goto*, Tsutomu Hirose

Department of Applied Chemistry, Kumamoto University, Kumamoto 860, Japan

First received 18 March 1994; revised manuscript received 25 May 1994

Abstract

The adsorption behaviour of two kinds of proteins, myoglobin and ovalbumin, with a membrane adsorber, DEAE MemSep 1000 (Millipore), was studied in comparison with a bead-based packed-bed adsorber, DEAE Sephacel (Pharmacia–LKB), by means of frontal analysis. Adsorption isotherms were obtained by integrating the breakthrough curves for various feed concentrations. Adsorption isotherms were expressed by the Langmuir equation and the adsorption capacity for the membrane adsorber was smaller than that for the packed-bed adsorber. The breakthrough curves of myoglobin for the membrane adsorber were independent of the flow-rate, but those of ovalbumin were affected by the flow-rate. Abnormal behaviour was observed for the adsorption of ovalbumin on a membrane adsorber. With the packed-bed adsorber, the breakthrough curves for both proteins were significantly affected by the flow-rate. A mathematical model for the membrane adsorber involving axial dispersion and adsorption kinetics was derived. The model simulated the breakthrough curves for myoglobin well. Axial dispersion was dominant for the membrane adsorber whereas intraparticle diffusion was dominant for the packed-bed adsorber.

1. Introduction

Downstream processes such as extraction, concentration, separation and purification are key techniques for the production of biological macromolecules such as enzymes, proteins and antibodies. Especially separation and purification play an important role in downstream treatment processing for biochemistry and biotechnology [1]. Considerable efforts have been devoted to the optimization of conventional methods and the development of new methods based on new principles in order to increase the productivity of separation and purification processes.

Liquid column chromatography is one of the most popular techniques for protein separation and purification and has been widely used in various fields of biotechnology from HPLC analysis to industrial-scale processes, because it is possible to purify proteins without losing their biological activity and to operate with simple equipment under mild conditions. Conventional bead-based packed-bed operation in column chromatography is carried out by pumping the feed solution to the packed bed containing porous particles. Packed-bed operation is not

* Corresponding author.

0021-9673/94/$07.00
SSDI 0021-9673(94)00493-S

necessarily the most suitable method for dealing with a large amount of dilute protein solution. Efficient adsorption can be realized when the breakthrough curve is steep with a high flow-rate resulting from a large overall adsorption rate which includes adsorbate–adsorbent association kinetics and mass transfer. The overall adsorption rate of protein is generally slow because of the large mass transfer resistance. With large porous particles, diffusion pathways for the proteins are relatively long and therefore low flow-rates are required to suppress kinetic effects. This causes long cycle times and inefficient operation in terms of operation time. On the other hand, efficient utilization of the adsorber can be attained when smaller particles of adsorbent are used because the dynamic adsorption capacity increases owing to the steep breakthrough. However, smaller particles make it difficult to operate at higher flow-rates owing to the high pressure drop [2], resulting in lower productivity. Therefore, an alternative technique to the packed-bed operation has been developed for preparative operation.

A membrane adsorber has been used to bypass these fundamental limitations of the packed-bed adsorber [2–5]. The ligands are immobilized on the surface of the membrane pores. The pores are designed to be large enough to permit convective flow. The overall adsorption rate may be large and steep breakthrough is expected because it is not affected by diffusion due to the convection through the pores of the membrane. Thus, mass transfer and pressure drop limitations could be minimized. Therefore, it is possible to operate at lower pressure drops, higher flow-rates and short cycle times. The membrane adsorber may allow the rapid processing of large volumes of feed stream and may be suitable for the separation and purification of large amounts of dilute protein solutions.

Membrane modules reported in the literature are classified into two types, stacked flat-sheet membranes or hollow fibre membranes. Brandt et al. [2] prepared an affinity membrane in a stacked membrane module. They demonstrated the efficient isolation of fibrinogen an immunoglobulin G with gelatin- and protein A-containing membranes. Liu and Fried [6] measured breakthrough curves of lysozyme through a stacked affinity membrane of cellulose–Cibacron Blue. Kim et al. [7] prepared a hollow fibre affinity membrane. The adsorption and elution behaviour of bovine γ-globulin with an affinity membrane containing hydrophobic amino acids as ligands was studied. These experimental studies revealed that the breakthrough curves were not influenced by the flow-rate. Hence diffusion resistance of a solute can be eliminated by convective flow through pores in the membrane.

Models of membrane adsorbers have been studied with regard to breakthrough analysis. A mathematical model including axial diffusion and adsorption kinetics was developed by Suen and Etzel [3], and was subsequently extended to multi-component systems [4]. Liu and Fried [6] developed a model including radial diffusion in addition to axial diffusion.

The membrane adsorber might suffer from heterogeneity of the membrane, that is, variation of the pore-size distribution, membrane thickness distribution, porosity distribution, etc., because of the short pathway in the flow direction. Suen and Etzel [3], Liu and Fried [6] and Goto and Hirose [8] have pointed out that the effect of heterogeneity is significant for a membrane adsorber.

The objective of this study was to investigate the adsorption behaviour of proteins with a membrane adsorber in comparison with a packed-bed adsorber. Two kinds of proteins, myoglobin and ovalbumin, were used as adsorbates. Breakthrough curves for each adsorber were measured and adsorption isotherms were obtained by integrating the breakthrough curves. The breakthrough curves and adsorption isotherms for the membrane adsorber were compared with those for the packed-bed adsorber. Mathematical models for each adsorber were derived and compared with the experimental results.

2. Model equations for breakthrough curve calculation

2.1. Model for a packed-bed adsorber

The breakthrough curves for a packed-bed adsorber may be described by the following model, containing rate processes of intraparticle and external film mass transfer resistance, axial dispersion and local adsorption kinetics. Some of these rate processes may cause broadening of the breakthrough curve.

The mass balance over a section of adsorber is expressed as

$$\varepsilon \cdot \frac{\partial c}{\partial t} + \varepsilon v \cdot \frac{\partial c}{\partial z} = \varepsilon D \cdot \frac{\partial^2 c}{\partial z^2} - (1-\varepsilon) a_p k_f (c - c_i|_{r=r_0}) \quad (1)$$

where c and c_i are the concentration in interparticle void space and in the pore of particle, respectively, and D and k_f denote axial dispersion coefficient and external film mass transfer coefficient, respectively. A mass balance within a particle is given by

$$\varepsilon_i \cdot \frac{\partial c_i}{\partial t} = D_e \cdot \frac{1}{r^2} \cdot \frac{\partial}{\partial r}\left(r^2 \cdot \frac{\partial c_i}{\partial r}\right) - \frac{\partial q}{\partial t} \quad (2)$$

where D_e and q are intraparticle effective diffusivity and the amount adsorbed, respectively. The association rate between adsorbate and adsorbent may be expressed by second order in the forward direction and first order in the revere direction [9]:

$$\frac{\partial q}{\partial t} = k_a c_i (q_\infty - q) - k_d q \quad (3)$$

where k_a, k_d and q_∞ are adsorption and desorption rate constants and maximum adsorption capacity, respectively. Eq. 3 is the rate equation which reduces to the Langmuir isotherm at equilibrium.

The initial and boundary conditions are

$$D_e \cdot \left.\frac{\partial c_i}{\partial r}\right|_{r=r_0} = k_f (c - c_i|_{r=r_0}) \quad \text{at } r = r_0 \quad (4)$$

$$\left.\frac{\partial c_i}{\partial r}\right|_{r=0} = 0 \quad \text{at } r = 0 \quad (5)$$

$$c = q = c_i = 0 \quad \text{at } z \geq 0, t = 0 \quad (6)$$

$$\varepsilon v c - \varepsilon D \cdot \frac{\partial c}{\partial z} = \varepsilon v c_0 \quad \text{at } z = 0, t > 0 \quad (7)$$

$$\frac{\partial c}{\partial z} = 0 \quad \text{at } z = L, t > 0 \quad (8)$$

where c_0 is the feed concentration of protein for step input.

Using the linear driving force (LDF) approximation [10], Eqs. 1–8 reduce to

$$\varepsilon \frac{\partial c}{\partial t} + \varepsilon v \cdot \frac{\partial c}{\partial z} = \varepsilon D \cdot \frac{\partial^2 c}{\partial z^2} - (1-\varepsilon) a_p k_p (c - \overline{c_i}) \quad (9)$$

$$\varepsilon_i \cdot \frac{\partial \overline{c_i}}{\partial t} = a_p k_p (c - \overline{c_i}) - \frac{\partial \bar{q}}{\partial t} \quad (10)$$

$$\frac{\partial \bar{q}}{\partial t} = k_a \overline{c_i} (q_\infty - \bar{q}) - k_d \bar{q} \quad (11)$$

$$c = \bar{q} = \overline{c_i} = 0 \quad \text{at } z \geq 0, t = 0 \quad (12)$$

$$\varepsilon v c - \varepsilon D \cdot \frac{\partial c}{\partial z} = \varepsilon v c_0 \quad \text{at } z = 0, t > 0 \quad (13)$$

$$\frac{\partial c}{\partial z} = 0 \quad \text{at } z = L, t > 0 \quad (14)$$

where $Bi = k_f r_0 / D_e$ and $a_p = 3/r_0$. The overall mass transfer coefficient, k_p, is given by $k_p = k_f/(1 + Bi/5)$, where intraparticle diffusion and external mass transfer effects are combined. $\overline{c_i}$ and $\bar{q}$ are average values of c_i and q, respectively.

Eqs. 9–14 were solved numerically using the finite-difference method for the simulation of breakthrough curves for a packed-bed adsorber.

2.2. Model for a membrane adsorber

In a membrane adsorber, intraparticle and external mass transfer resistance may be negligible because of convection through the pores of the membrane. Therefore, the model for the membrane adsorber is derived by excluding the terms of these mass transfer resistance from the

above model for the packed-bed adsorber. The resulting rate processes contain only axial dispersion and adsorption kinetics. The model equations derived are identical with the model of Suen and Etzel [3].

$$\varepsilon \cdot \frac{\partial c}{\partial t} + \varepsilon v \cdot \frac{\partial c}{\partial z} = \varepsilon D \cdot \frac{\partial^2 c}{\partial z^2} - (1-\varepsilon)\frac{\partial q}{\partial t} \quad (15)$$

$$\frac{\partial q}{\partial t} = k_a c(q_\infty - q) - k_d q \quad (16)$$

Liu and Fried [6] developed a model involving both radial dispersion and axial dispersion. As radial dispersion is less important than axial dispersion, it is neglected here. Eqs. 15 and 16, with initial and boundary conditions, Eqs. 6–8, were solved numerically by using the finite-difference method based on Crank–Nicholson's differencing scheme for the simulation of breakthrough curve for a membrane adsorber.

2.3. Calculation of breakthrough curve

The equations for the packed-bed and the membrane adsorbers were solved on a PC to simulate the adsorption processes.

The values of the maximum adsorption capacity q_∞ and equilibrium constant K_d $(=k_d/k_a)$ were determined from the experimental adsorption isotherms. Kinetic parameters involved in the model equations, overall mass transfer coefficient k_p, axial Peclet number Pe $(=vL/D)$ and adsorption rate constant k_a, were evaluated by fitting with the experimental breakthrough curves in the following procedure.

For the packed-bed adsorber, it was assumed as an initial guess that the value of Pe was 80, which corresponds to a particle Peclet number $vd_p/D = 0.5$ [11], and the value of k_a was infinite (or sufficiently large). Then k_p was determined by fitting the experimental data for the highest flow-rate, because broadening of the curve may be controlled by intraparticle diffusion for higher flow-rates. Theoretical curves for other flow-rates were calculated using the same parameters. If the calculated curve with those parameters did not agree with the experimental data for lower flow-rates, the calculations were repeated with modified parameters of Pe or k_a until they agreed with the experimental data.

In the case of the membrane adsorber, it was assumed as an initial guess that k_a was infinite (or sufficiently large) and axial dispersion caused the broadening of the breakthrough curve. The value of Pe was determined in the same way as for the packed-bed adsorber. If the calculated curve did not agree with the experimental curve for the entire flow-rate range, the value of k_a was decreased.

3. Experimental

Adsorption breakthrough curves were measured at 277 K for two kinds of anion exchanger: (a) an adsorber consisting of a stack of membrane, DEAE MemSep 1000 (Millipore), and (b) an adsorber packed with spherical beads, DEAE Sephacel (Pharmacia–LKB). The physical properties of the adsorbers are summarized in Table 1. Both adsorbers had the same volume. The membrane adsorber consisted of a multilayer microporous membrane assembled within the housing as shown in Fig. 1.

Myoglobin (horse heart; Sigma) and ovalbumin (Sigma) were used as adsorbates. The molecular mass and isoelectric point for myoglobin are 17 800 and 7.3, respectively, and those for ovalbumin are 46 000 and 4.6, respectively.

The breakthrough curves for these adsorbers were measured using the following procedure. First, the adsorber was equilibrated with 0.02 *M* Tris buffer solution. The pH of the buffer solution was adjusted with HCl to 9.3 and 8.0 for myoglobin and ovalbumin, respectively. The protein dissolved in the buffer solution was pumped to the adsorber until the available capacity of the adsorber was exhausted and the adsorbate concentration in the effluent of the adsorber approached the feed concentration. The effluent concentration was continuously monitored with a UV–Vis spectrophotometer at 533 and 280 nm for myoglobin and ovalbumin, respectively. The adsorbed protein was eluted with an eluent consisting of the buffer solution containing 1 *M* NaCl. The adsorber was finally

Table 1
Properties of adsorbers

Parameter	DEAE MemSep 1000 membrane adsorber	DEAE Sephacel packed-bed adsorber
Matrix	Cellulose	Cellulose
Pore size (m)	$1.2 \cdot 10^{-6}$	–
Porosity	0.8	–
Average particle diameter (m)	–	$1.0 \cdot 10^{-4}$
Column diameter (m)	$1.8 \cdot 10^{-2}$	$1.04 \cdot 10^{-2}$
Column height (m)	$5.0 \cdot 10^{-3}$	$16 \cdot 10^{-3}$
Bed volume (m^3)	$1.4 \cdot 10^{-6}$	$1.4 \cdot 10^{-6}$

equilibrated with the buffer solution for the next measurement.

4. Results and discussion

Fig. 2 shows adsorption isotherms of myoglobin and ovalbumin for the membrane adsorber, DEAE MemSep 1000, and Fig. 3 those for the packed-bed adsorber, DEAE Sephacel. The adsorption isotherms were obtained by integrating breakthrough curves measured at various feed concentrations at a flow-rate of $1.67 \cdot 10^{-8}$ m^3/s. The total adsorption capacity is generally independent of the flow-rate. As will be discussed later, the adsorption capacity for ovalbumin on the membrane adsorber depended on the flow-rate.

Each adsorption isotherm was expressed by a

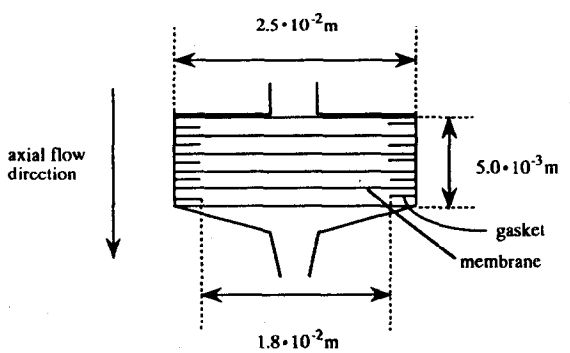

Fig. 1. Schematic diagram of a stack of membranes (DEAE MemSep 1000).

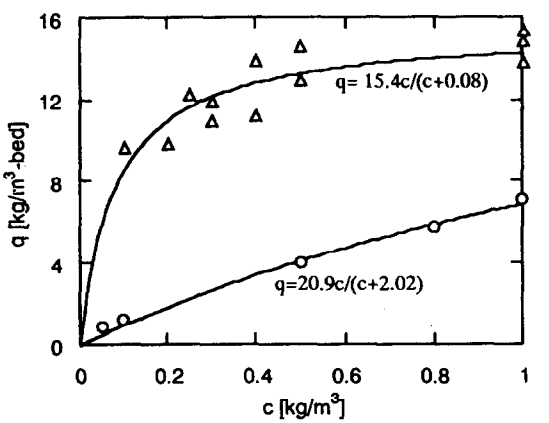

Fig. 2. Adsorption isotherms of (○) myoglobin and (△) ovalbumin for the DEAE MemSep 1000 membrane adsorber.

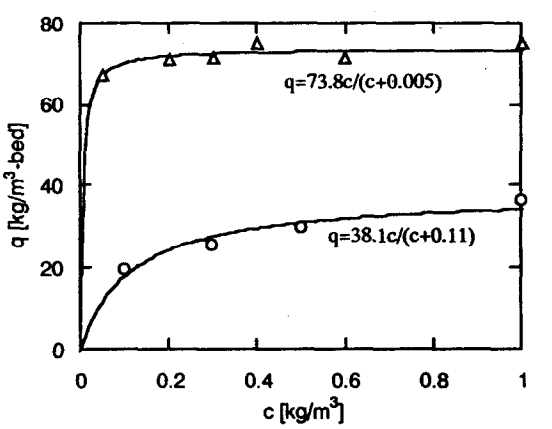

Fig. 3. Adsorption isotherms of (○) myoglobin and (△) ovalbumin for the DEAE Sephacel packed-bed adsorber.

Langmuir equation. The Langmuir constants, q_∞ and K_d, were determined by the least-squares method. The Langmuir equation is also shown in Figs. 2 and 3. Being compared on a mass basis of the adsorbate per unit volume of the adsorber, the amount adsorbed for the membrane adsorber was smaller than that for the packed-bed adsorber. The amount of myoglobin adsorbed was smaller than that of ovalbumin.

The effects of flow-rate on the breakthrough curve of myoglobin and ovalbumin for the membrane adsorber are shown in Fig. 4a and b, respectively. The theoretical breakthrough curves calculated by the model are also shown. The ordinate and abscissa are the ratio of effluent concentration to feed concentration and the ratio of effluent volume to bed volume, respectively. The adsorption breakthrough curves of myoglobin were steeper than those of ovalbumin. They were independent of flow-rate because of convection through the pores of the membrane, resulting in negligible diffusion resistance. The mathematical model for myoglobin nearly agreed with the experimental data when the value of *Pe* was 65 with an infinite value of k_a. On the other hand, the breakthrough curves of ovalbumin depended on flow-rate, especially for the highest flow-rate. The theoretical curves did not agree with the experimental data with any parameters. The dependence of the adsorption capacity on the flow-rate could not be represented by the model.

Fig. 5 shows the effect of flow-rate on the adsorbed amount calculated by integration of the curves after complete breakthrough. The data are plotted as amount adsorbed per unit bed volume against volumetric flow-rate. A larger amount of ovalbumin was adsorbed as the flow-rate increased. This abnormal behaviour cannot be explained by conventional adsorption theory. Kim et al. [7] stated the possibility of a flow-rate effect on adsorption for a membrane adsorber. The deformation of protein by shear stress might

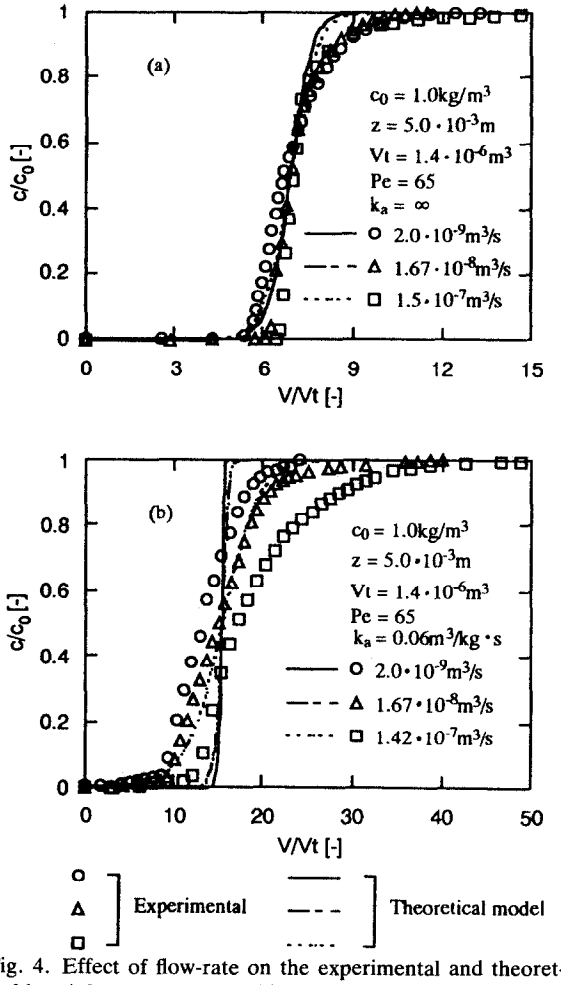

Fig. 4. Effect of flow-rate on the experimental and theoretical breakthrough curves of (a) myoglobin and (b) ovalbumin for the DEAE MemSep 1000 membrane adsorber.

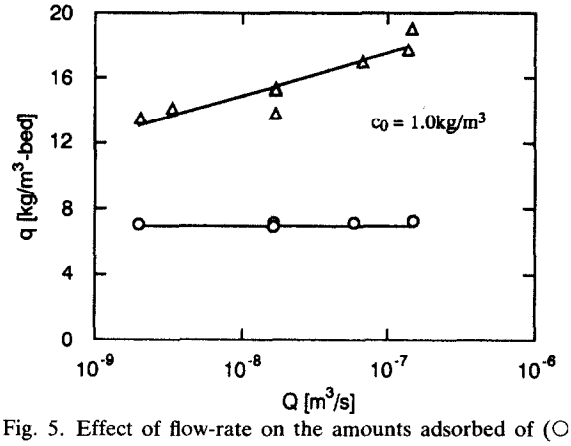

Fig. 5. Effect of flow-rate on the amounts adsorbed of (○) myoglobin and (△) ovalbumin for the DEAE MemSep 1000 membrane adsorber.

affect the adsorption. An effect of flow-rate on adsorption capacity was not observed for bovine γ-globulin on a phenylalanine- or tryptophan-containing membrane system under their experimental conditions. Skidmore et al. [12] observed that bovine serum albumin (BSA) had a higher adsorption capacity for a packed bed than expected from the adsorption isotherm obtained in stirred-tank experiments. This behaviour was not observed for lysozyme. They explained that this was due to multi-layer binding of BSA resulting from the formation of dimers. The dimer formation could be promoted by the flow which brings fresh BSA solution to the adsorbed protein. Therefore, the greater amount adsorbed at higher flow-rates observed in this work might be explained by multi-layer binding of ovalbumin molecules to molecules that are already adsorbed or dimerization of molecules or the influence of protein deformation due to the shear stress of the convective flow in the pores.

Heterogeneities of the membrane such as porosity distribution, thickness distribution and non-uniform flow through the membrane may exist [3,6,8]. Suen and Etzel [3] calculated the breakthrough curves when the membrane thickness and porosity had variations of 10%. They pointed out that even relatively small variations degrade the membrane performance [3]. The model containing these effects may also explain the broadening of the breakthrough curve of ovalbumin for higher flow-rates in the case of the membrane adsorber. When a larger number of membrane sheets are stacked, the influence of heterogeneity of the membrane may become less important.

Another important factor leading to broadening of curves may be non-ideality in the membrane module which includes non-uniform and uneven distribution of flow, leakage along the side of the membranes, variation of space between membranes and dead space in the housing. As mentioned by Liu and Fried [6], this effect is significant in membrane adsorbers.

The effects of flow-rate on the breakthrough curve of both proteins for the packed-bed adsorber are shown in Fig. 6a and b. The breakthrough curves of both proteins were signifi-

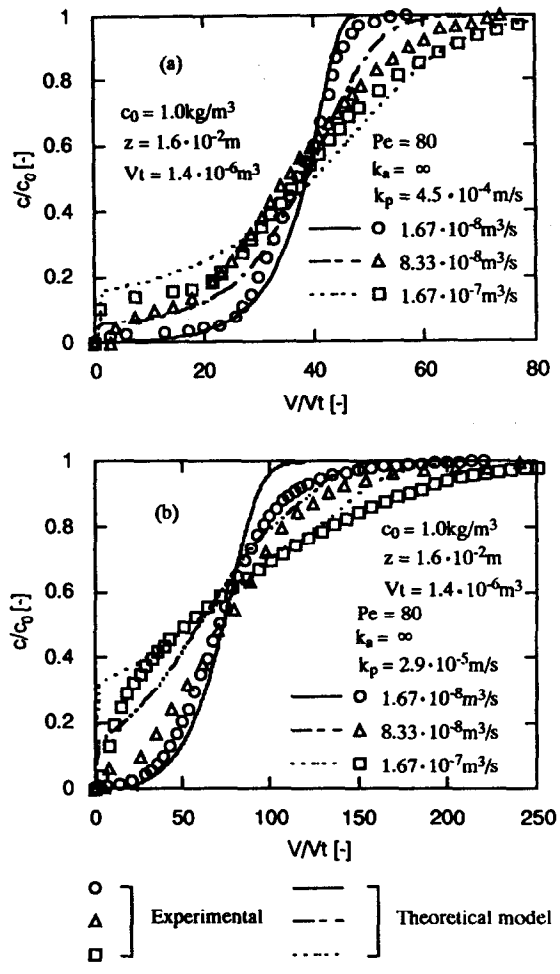

Fig. 6. Effect of flow-rate on the experimental and theoretical breakthrough curves of (a) myoglobin and (b) ovalbumin for the DEAE Sephacel packed-bed adsorber.

cantly affected by the flow-rate. This indicates the influence of the intraparticle diffusion resistance. The breakthrough curves of myoglobin were steeper than those of ovalbumin, mainly because the adsorption capacity of myoglobin is lower than that of ovalbumin and the diffusivity of myglobin is larger than that of ovalbumin owing to the difference in molecular mass. The abnormal behaviour of ovalbumin observed for the membrane adsorber was not observed for the packed-bed adsorber. The difference between the membrane adsorber and the packed-bed adsorber is the transport mechanism within the

Table 2
Parameters used in the calculation of mathematical models for packed-bed and membrane adsorbers

Protein	Parameter	Packed-bed adsorber	Membrane adsorber
Myoglobin	Pe	65	80
	k_a(m^3/kg·s)	∞	∞
	k_p(m/s)	$4.5 \cdot 10^{-4}$	–
Ovalbumin	Pe	65	80
	k_a(m^3/kg·s)	∞	0.06
	k_p(m/s)	$2.9 \cdot 10^{-5}$	–

adsorbent. The adsorbate molecule is transported to the adsorption site by diffusion for the packed-bed adsorber, whereas it is transported directly by the convective flow for the membrane adsorber. Therefore, liquid flow in the void space of particles does not affect on the adsorption behaviour within the particles. The breakthrough curves were simulated well by the model for the entire flow-rate range.

Table 2 summarizes the parameters estimated by fitting with experimental data. Although the modelling was not successful for the ovalbumin–membrane system, the parameters for the system are listed. In this work, association kinetics between adsorbate and adsorbent were not dominant because the association mechanism was ion exchange in the membrane used here. However, the association between solute and ligand for affinity adsorption may be slower and more important for the membrane adsorber owing to the absence of mass transfer resistance.

5. Conclusions

The breakthrough curves for the membrane adsorber were compared with those for the packed-bed adsorber. The amount adsorbed for the membrane adsorber was smaller than that for the packed-bed adsorber based on a unit volume of the adsorber. The breakthrough curves for the membrane adsorber were steeper than those for the packed-bed adsorber owing to convection through the pores of the membrane, leading to negligible diffusion resistance. For the packed-bed adsorber, the breakthrough curves were significantly affected by the flow-rate because of intraparticle diffusion resistance.

The breakthrough curves of myoglobin for the membrane were steeper than those of ovalbumin and independent of flow-rate; however, those of ovalbumin were affected by flow-rate. The mathematical model simulated well for myoglobin but not for ovalbumin.

Symbols

a_p specific surface area (m^{-1})
Bi $= k_f r_0 / D_e$; Biot number
c concentration in fluid phase (kg/m^3)
c_0 feed concentration (kg/m^3)
c_i concentration in fluid phase in pore (kg/m^3)
$\overline{c_i}$ average value of c_i (kg/m^3)
D axial dispersion coefficent (m^2/s)
D_e intraparticle effective diffusivity (m^2/s)
k_a adsorption rate constant (m^3/kg·s)
k_d desorption rate constant (s^{-1})
k_f external film mass transfer coefficient (m/s)
k_p overall mass transfer coefficient (m/s)
K_d desorption equilibrium constant (kg/m^3)
L column height (m)
Pe $= vL/D$; Peclet number
q amount adsorbed (kg/m^3)
q_∞ adsorption capacity (kg/m^3)
$\bar{q}$ average value of q (kg/m^3)
Q volumetric flow-rate (m^3/s)
r radial coordinate in a particle (m)
r_0 radius of a particle (m)
t time (s)
v interstitial velocity (m/s)
V effluent volume (m^3)

V_t bed volume (m^3)
z axial distance (m)
ε bed voidage or membrane porosity
ε_i porosity of a particle

Acknowledgement

This work was supported by a Grant-Aid for Scientific Research (No. 05750693) from the Ministry of Education, Science and Culture, Japan.

References

[1] S. Yamamoto and Y. Sano, *J. Chromatogr.*, 597 (1992) 173.
[2] S. Brandt, R.A. Goffe, S.B. Kessler, J.L. O'Conner and S.E. Zale, *Bio/Technology*, 6 (1988) 779.
[3] S.Y. Suen and M.R. Etzel, *Chem. Eng. Sci.*, 47 (1992) 1355.
[4] S.Y. Suen, M. Caracotsios and M.R. Etzel, *Chem. Eng. Sci.*, 48 (1993) 1801.
[5] K.G. Briefs and M.R. Kula, *Chem. Eng. Sci.*, 47 (1992) 141.
[6] H.-C. Liu and J.R. Fried, *AIChE J.*, 40 (1994) 40.
[7] M. Kim, K. Saito, S. Furusaki, T. Sato, T. Sugo and I. Ishigaki, *J. Chromatogr.*, 585 (1991) 45.
[8] M. Goto and T. Hirose, *J. Chem. Eng. Jpn.* 26 (1993) 523.
[9] F.H. Arnold and H.W. Blanch, *J. Chromatogr.*, 355 (1986) 13.
[10] M. Goto, J.M. Smith and B.J. McCoy, *Chem. Eng. Sci.*, 45 (1990) 443.
[11] O. Levenspiel, *Chemical Reaction Engineering*, Wiley, New York, 2nd ed., 1972.
[12] C.L. Skidmore, B.J. Horstmann and H.A. Chase, *J. Chromatogr.*, 498 (1990) 113.